v. 2, n. 2, 2025

International Journal of
Exact
Sciences

INTERSECTION OF GEODESIC ARCS FOR THE BENEFIT OF E-NAVIGATION REALITY

Ricardo Ramos Freire
IEAPM Head of Oceanography Department

Gilberto de Jesus de Oliveira
IEAPM Head of the Chemical Oceanography and Environmental Geochemistry Division

Alex Bolhosa Ferreira
IEAPM Head of Bioacoustics Division

Amilcar Mangueira Aguilar Junior
IEAPM Bioacoustics Division Assistant

Acceptance date: 30/04/2025

Abstract: This paper reflects on the new S-100 reality and offers a calculation algorithm for determining the intersection between geodesic lines on the ellipsoidal reference surface according to the accuracies expected in nautical cartographic products.
Keywords: Ellipsoid, e-Navigation, intersection, geodesic lines, and S-100.

INTRODUCTION

The advent of computer-aided cartography (CAC) impacted the cartographic representation of objects of interest for the safety of navigation, allowing analog products to evolve into the reality of line vectorization. It was a paradigm shift, where operators needed to assimilate new skills to work with CAC - from the point of view of the products (paper charts and later raster charts), there was no significant qualitative evolution.

Using computers to update nautical charts only made a real impact with the advent of Electronic Navigational Charts (ENC); topological integrity, quality controls, and the eventual use of spatial databases revealed previously unknown shortcomings of paper (and raster) charts.

Before ENCs, the verification performed by CAC editors consisted of the visual inspection of printed products. Control processes accepted open or discontinuous polygons, vertical inconsistencies between products of different compilation scales, and improper cartographic generalization processes, among many other problems, including those of topological nature. A single chart may have more than 3,000 objects and the Brazilian Directorate of Hydrography and Navigation (DHN) portfolio consists of several hundred paper charts, one can acknowledge that this was a significant problem. Hence, DHN conducted a major effort to correct the errors and generate the ENC cells.

The problems identified were not exclusive to Brazil. The encoding of ENCs, based on the International Hydrographic Organization (IHO) standard S-57 (IHO Transfer Standard for Digital Hydrographic Data), impacted the entire international community. To improve product quality, the IHO created Annex C of Appendix B.1 of S-57, establishing the first quality controls. This annex has been discontinued and replaced by what cartographic engineers (the name of mapping professionals in Brazil) know as the S-58 standard (ENC Validation Checks). This compendium of logical and topological consistency tests, among others, aimed to improve the geometric aspect of the coded features and the relationships between these features, including metadata, increasing the coherence of the ENC. Software manufacturers began to develop tools to build ENCs based on S-57 and run the respective quality controls derived from the S-58 rules. The production flow naturally evolved to primarily update the ENC databases and cells (with their respective controls) and then, in a derivative way, update the paper and raster charts.

The international community is once again experiencing a period of inflection with e-Navigation. At the backbone of this process, the new IHO Universal Hydrographic Data Model (S-100) is developing a common framework for several new geospatial standards that benefit the maritime community. Dozens of new standards are in the pipeline, aiming for a much more complete navigation planning, execution, verification, and correction experience (yes, as in PDCA!) than the ENC cells, based on S-57, could provide. The IHO has taken over standards S-101 to S-199, ranging from the new electronic nautical chart (S-101, ENC Product Specification) to bathymetric surfaces (S-102, Bathymetric Surface Product Specification), tides (S-104, Water Level Information for Surface Navigation Product Specification), surface currents (S-

111, Surface Currents Product Specification), etc. Because of the complexity, several other organizations are contributing (or planning to contribute) to the development of specific standards, such as the International Association of Marine Aids to Navigation and Lighthouse (IALA) (S-201 to S-299), Intergovernmental Oceanographic Commission (IOC) (S-301 to S-399), Inland ENC Harmonization Group (IEHG) (S-401 and S-402), WMO Service Commission (SERCOM) (S-411 to S414), International Electrotechnical Commission - TC80 (IEC-TC80) (S-421 to S-430) and NATO Geospatial Maritime Working Group (GMWG) for Additional Military Layers (AML) (S-501 to 525). Some modifications introduced in the S-100 framework will change the construction rigor of nautical cartography products. The following discussion presents one of these aspects.

S-57 TO S-100

The evolution of S-57 data modeling to S-101 (ENC Product Specification), which is subordinate to the S-100 framework, is relatively complex, the paper does not intend to exhaust the subject, presenting topics regarding interpolation methods for line segments.

The first aspect to highlight is item 2.1.7 of Annex A, Appendix B.1 of the S-57 standard defines the Coordinate Multiplication Factor (COMF) parameter will always be 10^7, meaning that the latitude and longitude coordinates of the ENC cells, based on the S-57, will have their values stored up to the 7th decimal place, which would be equivalent to 11.132 mm at the Equator, considering the GRS-80 bi-axial ellipsoid - this imposition does not depend on the bands of use, nor does it depend on the scale of compilation of each cell. Additionally, in Annex B of S-65 (S-57 ENC to S-101 Conversion Guidance), item 2.1.7, the COMF value is retained for S-101 but stores the data set structure information (DSSI) field in subfields CMFX and CFMY - this specification is in item 10.1.1 of the S-101.

Returning to S-57, item 7.7.1.8 presents the types of arc/curve interpolation: Arc 3 point center, Elliptical arc, Uniform B-spline, Piecewise Bezier, and Non-uniform rational B-spline. Item 9-7.2 of the S-100, we have: None, Linear, Loxodromic, Circular Arc 3 Points, Geodesic, Circular Arc Center Point with Radius, Elliptical, Conic, Polynomial Spline, Bezier Spline, B-Spline, and Blended Parabolic. Of these two lists, what is most striking is that almost all the interpolators rely on Euclidean geometry on projective systems, except one: the geodesic interpolator. Naturally, this interpolator is applied considering the ellipsoidal reference surface. More importantly, this specification is not in the S-101, but in the S-100. In other words, this interpolator applies to all standards. Note that navigation systems present ENC through projective systems as a resource for better understanding by the human navigator. In times of intelligent autonomous navigation systems, this limitation could fall by the wayside. What would prevent a navigation system from working with native geodesic coordinates (or even three-dimensional geocentric coordinates)? Absolutely nothing - it would be more consistent with the search for the shortest (unobstructed) route between two points. It's worth remembering that the use of the various layers of the S-100 by e-Navigation increases the need for interoperability between the products (something that S-98, Data Product Interoperability in S-100 Navigation Systems, seeks to harmonize) and the capacity for assimilation by the human navigator for their respective decision-making process. The provision of geodetic interpolators, which did not exist in the S-57, enhances the future of electronic navigation.

As mentioned earlier, the quality controls for ENCs based on the S-57 are in the S-58 standard. S-101 Annex C included a set of

International Journal of Exact Sciences ISSN 2966-1153 DOI https://doi.org/10.22533/at.ed.153222529041

quality control rules. At the 2023 meeting of the IHO Hydrographic Services and Standards Committee (HSSC15), there was a request for S-158 numbering allocation to S-100 validation checks (including S-98). S-158:101 Edition 1.0.0 release was in January 2025; its validation checks are like S-58 and focused on S-101. Another publication, S-158:100 (Universal Hydrographic Model Validation Checks) will hold the validation checks for all other S-100 products.

Finally, in item 1.4.2 of S-58, for all spatial operators (EQUALS, DISJOINT, TOUCHES, WITHIN, OVERLAPS, CROSSES, INTERSECTS, CONTAINS, and COINCIDENT) based on ISO 19125-1, a standard tolerance of 1/COMF must apply to validation software. This article presents a calculation algorithm for intersecting geodesic lines.

GEODESIC LINES

According to BOMFORD (1952), the smallest line segment joining two points on the ellipsoid of revolution is a segment of the geodesic line. With *N* being the radius of curvature of the first vertical section, *M* the radius of curvature of the meridian section, *ds* the surface differential, $d\phi$ latitude and $d\lambda$ longitude, the first fundamental form of the ellipsoid of revolution is expressed by (PEARSON, 1977):

$$ds^2 = (M \cdot d\phi)^2 + (N \cdot cos(\phi) \cdot d\lambda)^2$$

The values of M and N are:

$$M = \frac{a \cdot (1 - e1^2)}{\{1 - [e1 \cdot sen(\phi)]^2\}^{1,5}}$$

$$N = \frac{a}{\sqrt{1 - [e1 \cdot sen(\phi)]^2}}$$

The values of the semi-major axis a (6,378,160 m) and flatness f (1/298,257223563) define the GRS-80 ellipsoid, adopted as a reference by the World Geodetic System 1984 (WGS84), the horizontal reference datum for nautical charts. The first eccentricity *e1* is given by:

$$e1 = \sqrt{f \cdot (2 - f)}$$

One can define geodesic lines by the differential equations below:

$$\frac{d\phi}{ds} = \frac{cos(\alpha)}{M}$$

$$\frac{d\lambda}{ds} = \frac{sen(\alpha)}{N \cdot cos(\phi)}$$

$$\frac{d\alpha}{ds} = \frac{tan(\phi) \cdot sen(\alpha)}{N}$$

Where *a* is the geodetic azimuth.

The first fundamental form is the starting point for direct and inverse solutions adopted in this paper. The chosen method is that of VINCENTY (1975).

Given a bi-axial ellipsoidal reference surface, a geodesic line, in general, is not a plane curve. However, the plane containing three nearby points on any geodesic also contains the gradient to the ellipsoid at the center of those three points. The Meridians and the Equator are specific geodesic lines because they are flat curves. Orthodromic lines are geodesic lines (or maximum circles) for a spherical reference surface. These lines, however, are not geodesic lines for the ellipsoidal reference surface, which is the subject of this study.

DIRECT AND INVERSE GEODETIC CALCULATION

One may divide the solution to the geodesic lines problem into two parts:

- direct: from the geodesic coordinates of an origin point on the ellipsoid, determine the destination point, knowing the geodesic distance and azimuth between the points (Figure 1); and

- inverse: given the geodesic coordinates of two points, calculate the geodesic distance and azimuth between the points (Figure 2).

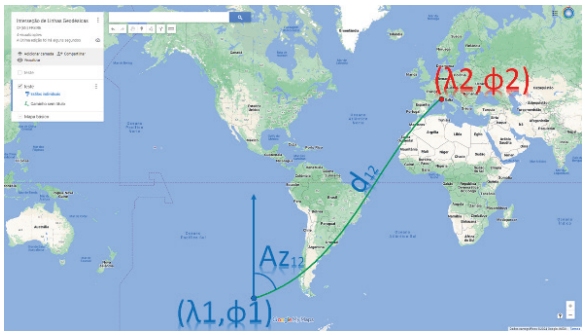

Figure 1: Direct solution for geodesic lines on the ellipsoid.

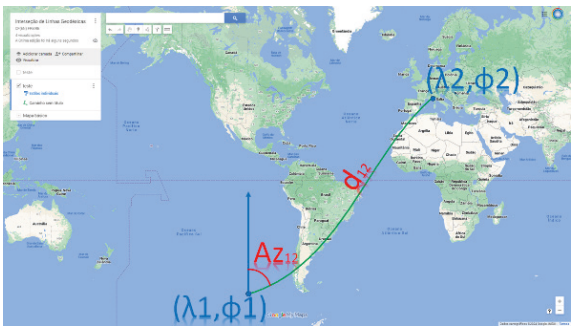

Figure 2: Inverse solution for geodesic lines on the ellipsoid.

The VINCENTY method (1975) is one of the best-known and most widely used due to its simplicity of implementation, the accuracy of results, and low computational cost. For this study, the method used the original expansion up to the u8 and B3 terms. In addition, the team adopted a convergence criterion of 10^{-20} for the longitudes in the indirect method and the same magnitude for converging the angular distances in the direct method. RAPP (1993) presents additional considerations on non-iterative methods and the geodesic behavior of antipodal points.

EXAMPLE OF CALCULATING THE COORDINATES OF THE POINT OF INTERSECTION BETWEEN TWO GEODESIC LINES

A pair of geodesic lines cross at point S. The first joins points 1 and 2 and the second joins points 3 and 4, as shown in Figure 3. The geodesic line segment joining points 1 and 2 has been defined as g_{12} and points 3 and 4 as g_{34}.

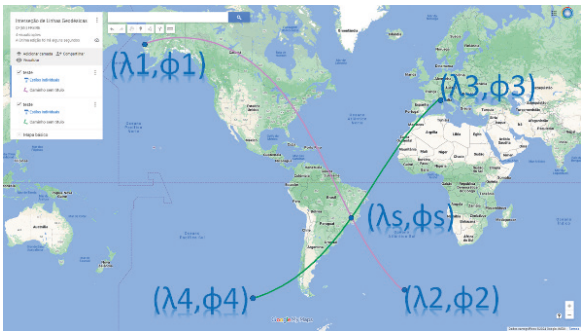

Figure 3 - the intersection between two geodesic lines

S-58 establishes that spatial operators must have a standard tolerance up to the 7th decimal place of the geodesic coordinates (and that this reality persists in the S-101 through S-158:101), this is the desirable precision for the method.

Points 1, 2, 3, 4, and S have the following coordinates:

P	Lat	Long
1	62,5856080º	-164,8953810º
2	-53,03254672407609º	-14,108183272619748º
3	43,7394160º	7,4195730º
4	-55,81656238317595º	-102,10055177300606º
S	-19,8802811º	-44,0125331º

Table 1 - Coordinates of the endpoints of the geodesic line segments and the point of intersection (calibration)

Points 1, 3, and S are for control purposes, from which it is possible to calculate the geodesic azimuths Az_{1S} and Az_{3S}. Using the respective azimuths, point 2 was established at 18,000 km from point 1 and point 4 at 15,000 km from point 3, using the direct method of VINCENTY (1975). This way, it will be possible to assess the accuracy of calculated coordinates at the intersection point of geodesic lines g_{12} and g_{34}.

If g_{12} and g_{34} were significantly shorter, it would be possible to establish a more user-friendly geometry to represent these geodesics, so that the intersection between them was algebraically determinable. One possible approach is to populate g_{12} and g_{34} with points

belonging to each geodesic line. To do this, take the coordinates of point 1 as the origin and, using the geodesic azimuth Az_{12}, calculate the coordinates of the points belonging to g_{12} every 1 m (step). The same procedure was for g_{34}. For g12, 18 million points, g34, 15 million. To identify the closest pair of points to the intersection solution, it would be necessary to evaluate 270 trillion options, which is inefficient.

We opted for a strategy of densifying the points of the geodesic lines with a variable step, as shown below for g_{12}:

- Calculates the distance between points 1 and 2;
- Calculates the number of points by truncating the division between the distance and the step;
- Calculates the azimuth of g_{12};
- Calculates the coordinates of the points belonging to g_{12} using the direct method of VINCENTY (1975).

The same procedure for g_{34}. With an initial step of 1,000 km, one can compare the two matrices of points on the geodesic lines to establish which pair of points (one on g_{12} and the other on g_{34}) has the smallest absolute sum of the difference between the coordinates. After identifying the two points, select the adjacent preceding and following points on g_{12} and g_{34}. With these new boundaries, the procedure is repeated, now with a step of 100 km. This process is repeated by successively downscaling by 1/10 until a 1-m step.

Then, one may evaluate the g_{12} coordinate matrix for linearity between latitudes and longitudes. Due to the values involved in this study, replacing the analysis of the coefficient of determination r^2 by the tolerance, defined as $1\text{-}r^2$, was an efficient way to present the linearization goodness.

For g_{12}, the tolerance was $9.73 \cdot 10^{-14}$. For g_{34}, the value is $9.90 \cdot 10^{-14}$.

Both values indicate high linearity between latitudes and longitudes on each geodesic line.

Selecting a linear model solves the issue, as shown below:

$$a \cdot \phi_n + b = \lambda_n$$

For g_{12} we have 20 equations while for g_{34} there are 21. To solve this system, the l2-norm is adopted, using the Least Squares Method:

$$\underbrace{\begin{pmatrix} \phi_0 & 1 \\ \vdots & \vdots \\ \phi_n & 1 \end{pmatrix}}_{A} \cdot \underbrace{\begin{pmatrix} a \\ b \end{pmatrix}}_{X} = \underbrace{\begin{pmatrix} \lambda_0 \\ \vdots \\ \lambda_n \end{pmatrix}}_{B}$$

$$X = (A^T \cdot A)^{-1} \cdot (A^T \cdot B)$$

The vector below describes the residuals of the parametric adjustment:

$$V = A \cdot X - B$$

The square root of the mean squared error is given by:

$$RMSE = \sqrt{\frac{V^T \cdot V}{n-1}}$$

When solving the system of equations, one obtains RMSE12 of $6.42 \cdot 10^{-4}$ degrees and $RMSE_{34}$ of $6.21 \cdot 10^{-4}$ degrees. These values are incompatible with the desired precision (7^{th} decimal place). Note that inverting the square of the Jacobian matrix A to obtain X often presents problems, depending on the nature of the data.

Note that RMSE can be related to the coefficient of determination (WEISSTEIN, 2017):

$$r^2 = 1 - \frac{V^T \cdot V}{\sum_{i=0}^{n-1} \left(B_i - \overline{B}\right)^2}$$

Rearranging, we have:

$$RMSE = \sigma_B \cdot \sqrt{1 - r^2}$$

σ_B is the standard deviation of B or the standard deviation of the subset of geodetic longitudes of g_{12} or g_{34}.

The advantage of this way of calculating the RMSE is that it is not necessary to determine the solution parameters of vector X to calcu-

late the residual vector V. This RMSE is not subject to the problems of matrix inversion of the squared Jacobian matrix A. $RMSE_{12}$ was $8.31 \cdot 10^{-12}$ degrees while the $RMSE_{34}$ was $1.08 \cdot 10^{-11}$ degrees, compatible with COMF, CMFX, and CMFY. Those RMSEs were encouraging enough to develop a viable solution compatible with those results. One can solve the matrix inversion problem by using the LU factorization method, as shown below:

$$A^T \cdot A = L \cdot U$$

$$A^T \cdot A \cdot X = A^T \cdot B$$

$$L \cdot U \cdot X = A^T \cdot B$$

$$L \cdot Y = A^T \cdot B$$

$$U \cdot X = Y$$

With the LU factorization, it was possible to calculate the solution vectors X_{12} and X_{34}, whose respective RMSE was $7.85 \cdot 10^{-9}$ degrees and $1.85 \cdot 10^{-9}$ degrees. With the solution vectors, it is possible to determine the coordinates of the intersection point of geodesics g_{12} and g_{34}. The values calculated were:

$$LatS = -19.880281102317355°$$

$$LongS = -44.01253310175605°$$

Since point S coordinates are at the beginning of the project, the associated errors are below:

$$\varepsilon_{LatS} = (2.32 \cdot 10^{-9})°$$

$$\varepsilon_{LongS} = (1.76 \cdot 10^{-9})°$$

CONCLUSION

The errors presented for the intersection between the geodetic lines at 18,000 km and 15,000 km, respectively, were 10^{-9} degrees order, compatible with the precision established in S-58 and S-100/S-101.

For future work, we recommend the VINCENTY(1975) method enhancement evaluation, expanding the series by more terms to assess its share in determining the geodesic intersection. Moreover, other decomposition methods, such as Cholesky, QR, Jordan, Hessenberg, etc., check for RMSE improvements.

REFERENCES

BOMFORD, G. Geodesy. New York. 1952.

IHO, S-57 Transfer Standard for Digital Hydrographic Data. https://iho.int/uploads/user/pubs/standards/s-57/31Main.pdf, 2000. Visited on 01/21/2025.

IHO, S-57 Appendix B.1, Annex A - Use of the Object Catalogue for ENC - UOC. https://iho.int/uploads/user/pubs/standards/s-57/S-57%20Appendix%20B.1%20Annex%20A_UOC_Ed%204.3.0_Final.pdf, 2022. Visited on 01/21/2025.

IHO, S-58 ENC Validation Checks. https://iho.int/uploads/user/pubs/standards/s-58/S-58%20Ed%207.0.0_Final.pdf, 2022. Visited on 01/21/2025.

IHO, S-65 Annex B S-57 ENC to S-101 Conversion Guidance. https://iho.int/uploads/user/pubs/standards/s-65/S-65%20Annex%20B_Ed%201.1.0_Final.pdf, 2023. Visited on 01/21/2025.

IHO, S-98 Data Product Interoperability in S-100 Navigation Systems. https://iho.int/uploads/user/pubs/standards/S-98/S-98%20Main_Ed%201.0.0_Final.pdf, 2022. Visited on 01/21/2025.

IHO, S-100 Universal Hydrographic Data Model. https://iho.int/uploads/user/pubs/standards/s-100/S-100_5.1.0_Final_Clean.pdf, 2023. Visited on 01/21/2025.

IHO, S-101 ENC Product Specification. https://registry.iho.int/productspec/view.do?idx=195&product_ID=S-101&statusS=5&domainS=ALL&category=product_ID&searchValue=, 2023. Visited on 01/21/2025.

IHO, S-101 Annex A_DCEG. https://registry.iho.int/productspec/view.do?idx=195&product_ID=S-101&statusS=5&domainS=ALL&category=product_ID&searchValue=, 2023. Visited on 01/21/2025.

IHO, S-101 Annex C_Validation Checks. https://registry.iho.int/productspec/view.do?idx=195&product_ID=S-101&statusS=5&domainS=ALL&category=product_ID&searchValue=, 2023. Visited on 01/21/2025.

IHO, S-102 Bathymetric Surface Product Specification. https://registry.iho.int/productspec/view.do?idx=199&product_ID=S-102&statusS=5&domainS=ALL&category=product_ID&searchValue=, 2023. Visited on 01/21/2025.

IHO, S-104 Water Level Information for Surface Navigation Product Specification. https://registry.iho.int/productspec/view.do?idx=198&product_ID=S-104&statusS=5&domainS=ALL&category=product_ID&searchValue=, 2023. Visited on 01/21/2025.

IHO, S-111 Surface Currents Product Specification. https://registry.iho.int/productspec/view.do?idx=178&product_ID=S-111&statusS=5&domainS=ALL&category=product_ID&searchValue=, 2023. Visited on 01/21/2025.

IHO, S-158:101 Electronic Navigational Chart Validation Checks. https://iho.int/uploads/user/pubs/standards/S-158_101/S-158-101_Validation_Checks_Ed_1.0.0.zip, 2025. Visited on 03/17/2025.

PEARSON, Frederick. Map Projection Equations. Naval Surface Weapons Center, Dahlgren Laboratory, 1977.

RAPP, Richard H. Geometric geodesy part 2. 1993.

VINCENTY, Thaddeus. Direct and inverse solutions of geodesics on the ellipsoid with application of nested equations. Survey review, v. 23, n. 176, p. 88-93, 1975.

WEISSTEIN, Eric W. Correlation coefficient. https://mathworld. wolfram. com/, 2006. Visited on 01/21/2025.